Available online at www.sciencedirect.com
ScienceDirect
Journal of Catalysis 246 (2007) 15–28
JOURNAL OF CATALYSIS
www.elsevier.com/locate/jcat

Mild electrocatalytic hydrogenation of lactic acid to lactaldehyde and propylene glycol

Tulika S. Dalavoy [a], James E. Jackson [a,*], Greg M. Swain [a], Dennis J. Miller [b], Jie Li [c], Jacek Lipkowski [c]

[a] *Department of Chemistry, Michigan State University, East Lansing, MI 48824, USA*
[b] *Department of Chemical Engineering and Materials Science, Michigan State University, East Lansing, MI 48824, USA*
[c] *Department of Chemistry and Biochemistry, University of Guelph, Guelph, ON N1G2W1, Canada*

Received 13 August 2006; revised 31 October 2006; accepted 1 November 2006

Available online 12 December 2006

Abstract

Reduction of fermentation-derived lactic acid (LA) offers a renewables-based pathway to propylene glycol (PG), a large-scale commodity chemical, currently manufactured by the oxidation of petroleum-derived propene. Complementing our previously described catalytic hydrogenation of LA to PG, we now report electrocatalytic hydrogenation (ECH) of LA in an aqueous electrolyte using constant current electrolysis. A reticulated vitreous carbon (RVC) electrode serves to agglomerate, support, and supply current to a 5% Ru/C powder catalyst, the same catalyst used in the classical hydrogenations. The ECH conditions are mild (ambient pressure, 70 °C vs 1500 psi H_2, 150 °C) relative to the chemical hydrogenation. More surprisingly, the major electrohydrogenation product is lactaldehyde (LAL), with small quantities of PG also formed. Variable current studies in the range of 10–100 mA show an increase in product yields and a shift in selectivity toward PG with increasing current. Experiments carried out with different acids as electrolytes reveal a distinct effect of the anion on the yields of the two products. In situ ATR-FTIR studies of the ECH of LA point to a chelating bidentate carboxylate adsorption mode for lactate on the Ru surface and offer insight into the effects of electrolyte anions on surface adsorption and reactivity.

Keywords: Electrocatalytic hydrogenation; Lactic acid; Lactaldehyde; Propylene glycol; Reticulated vitreous carbon; Organic electrochemistry; Electrosynthesis; Green chemistry; ATR; SEIRAS; FTIR

1. Introduction

Prompted by the long-term imperative to replace fossil hydrocarbons with renewable resources as the basis for the chemical and energy industries, the search is on for alternative paths to chemical building blocks from biomass-derived intermediates such as glucose, glycerol, and organic acids. In recent years, we described aqueous phase heterogeneous catalytic hydrogenation of lactic acid (LA; IUPAC name, 2-hydroxypropanoic acid) to propylene glycol (PG; IUPAC name, 1,2-propanediol), an important ($>10^9$ kg/year in the United States) commodity chemical used widely across industrial sectors. Although its yield is >95% in the presence of a 5% Ru/C catalyst in water, this conversion requires high temperature and pressure conditions (150 °C, 1200 psi H_2) [1]. Interestingly, lactic and α-amino acids have turned out to be especially favorable substrates, undergoing reduction substantially faster than unsubstituted propanoic acid [1,2]. Indeed, conditions severe enough to reduce simple alkanoic acids lead to degraded selectivities, as C–O and C–C bond hydrogenolyses begin to compete with carboxylate reduction. Because the overall heats of hydrogenation of the substituted and the parent carboxylic acids are almost equal, it appears that the α-OH or $-NH_3^+$ groups exert a kinetic influence independent of the underlying thermochemistry.

Electrocatalytic hydrogenation (ECH) offers a mild alternative to traditional chemical catalytic methods. Here the unsaturated organic compound (Y=Z) is reduced by hydrogen formed from electrolytic acid decomposition at the surface of an electrode made of catalytic metal, as shown in Scheme 1. Because

* Corresponding author. Fax: +1 517 353 1793.
E-mail address: jackson@chemistry.msu.edu (J.E. Jackson).

0021-9517/$ – see front matter
doi:10.1016/j.jcat.2006.11.009

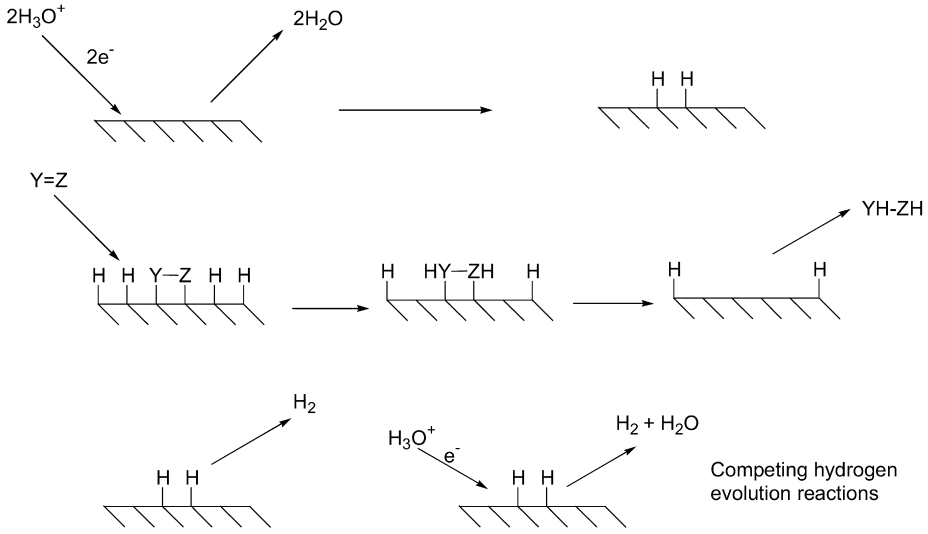

Scheme 1. Electrocatalytic hydrogenation and hydrogen evolution.

the hydrogen is produced in situ on the catalyst surface, this strategy eliminates three difficulties: (1) the need for high pressures to achieve adequate concentrations of (poorly soluble) hydrogen gas, (2) its mass transport, and (3) its splitting into hydrogen atoms on the catalyst surface. Compared with chemical catalytic hydrogenation, ECH should enable milder, and hence more selective, reaction. Safety would be improved as well; with no external hydrogen source required, the need to store and handle potentially hazardous high-pressure hydrogen gas would be obviated.

Although a number of authors have explored ECH of unsaturated substrates such as phenol [3,4], diketones [5], enones [6], and aldehydes [7], on electrodes such as Pt, Raney Ni, Raney Co, and Pd/carbon felt, to the best of our knowledge, no such studies have been reported for free carboxylic acids. The use of aqueous electrolyte mirrors our chemical catalytic studies, in which water was chosen as the native (and "greenest") medium for biomass-derived organic acids. We have since found that the aqueous environment is uniquely favorable; organic solvents generally degrade reaction rates and selectivities relative to those in water [8].

This project's long-term goal is a general process for large-scale, aqueous-phase stereoretentive[1] catalytic hydrogenation of renewables-derived carboxylic acids under temperature and pressure conditions milder than those of current state-of-the-art chemical conversions (batch or continuous). Electrochemistry is also amenable to in situ observation via attenuated total reflection (ATR) infrared and Raman spectroscopies, offering insights into the mechanistic details of metal-catalyzed hydrogenations. We have used such spectroelectrochemical techniques to probe the mode of binding of the substrate on the electrode surface, the nature of the intermediates formed during hydrogenation, and the mechanism by which the α-position functional groups can facilitate hydrogenation of carboxylic acids.

This paper describes a series of ECH studies of LA using a RVC electrode suffused with a powder catalyst. The same 5% Ru/C powder catalyst was used in our studies of the chemical catalytic hydrogenation [2], so the physical form of the catalyst, and presumably the essential components of the catalytic process, were retained, allowing maximum comparability between the new electrochemical and the chemical processes. The RVC's three-dimensional network of large pores provides electrically conductive host sites to support the powder catalyst particles. With a high overpotential for hydrogen evolution, it is an electrochemically stable support material and not itself expected to effect electrohydrogenation or water reduction, as our control experiments confirm. Previous work using this type of electrode was reported by Menard and coworkers [3,9–12] in the context of ECH of phenol and other organic compounds.

This work's unexpected finding is that lactaldehyde (2-hydroxypropanal) (LAL) is the major product instead of the expected PG, which only occasionally appears as a minor part of the product mixture. This thermodynamically surprising result apparently reflects the relative rates of reduction and surface desorption/adsorption, together with the aqueous hydration properties of the starting materials and the two products.

2. Experimental

S-LA and PG were purchased from Aldrich and were used without further purification. 5% Ru/C was purchased from PMC Catalysts.

2.1. Electrochemical cell setup

Electrohydrogenation studies of LA in several aqueous electrolyte solutions were carried out in the glass electrochemical cell depicted below (Fig. 1). It is a two-compartment cell with the anode and the cathode compartments separated by a glass frit to prevent the diffusion of gaseous products. The reference

[1] In the heterogeneous catalytic hydrogenation of chiral lactic acid [1], the high temperature and pressure causes some racemization at the stereocenter of lactic acid, lowering the enantiomeric excess to ∼90%. The rate of racemization decreases with decrease in temperature. The milder conditions of alanine hydrogenation [2] allow for completely stereoretentive reduction.

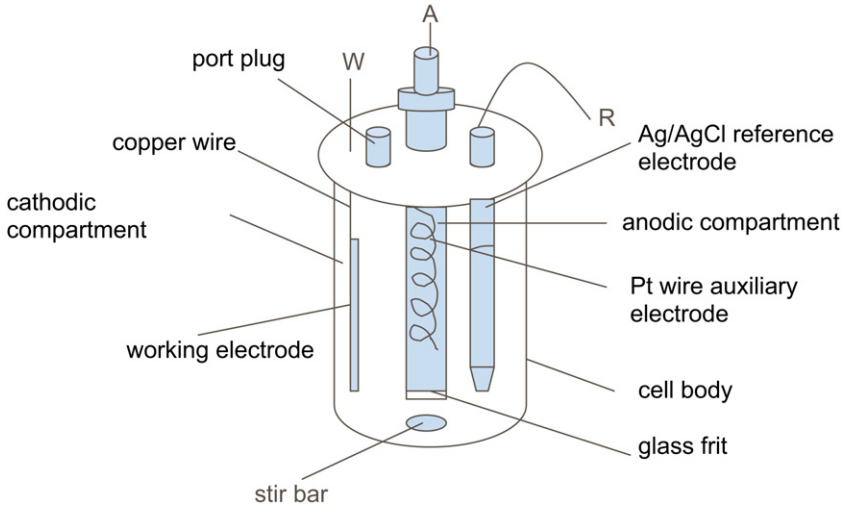

Fig. 1. Schematic diagram of the electrochemical cell.

electrode was Ag/AgCl ($E^0 = -0.35$ V vs SCE). The counter electrode is Pt wire. The RVC working electrode (dimensions $4.0 \times 3.0 \times 0.5$ cm; pore size, 100 pores per inch [ppi]) was connected to the external circuit via a copper wire, positioned to minimize surface area exposed to solution; electrochemistry on the copper surface can thus be assumed to be negligible. A voltmeter was connected between the reference and working electrode to measure the potential of the working electrode. Controlled current was applied using a model 273 potentiostat/galvanostat from EG&G Princeton Applied Research. The temperature of the system was controlled using a heating tape wrapped around the cell and connected to a temperature controller from Omega.

2.2. Electrocatalytic hydrogenation

Before each experiment, 1.0 g (dry weight) of 5% Ru/C was added to the electrolyte solution and the solution was stirred for 2 h under cathodic polarization ($I = 20$–40 mA) to ensure proper agglomeration of the catalyst in the pores of the RVC. The potential of the working electrode during this process was in the range of -100 to -400 mV (vs Ag/AgCl) depending on the electrolyte and the temperature of the cell. The stirring rate was kept low to prevent the agglomerated catalyst from being washed off the pores. The RVC surfaces before and after agglomeration were examined by scanning electron microscopy (SEM) as shown in Fig. 2. Elemental composition as measured via energy-dispersive spectral (EDS) analysis showed the average surface Ru content to be about $5.5 \pm 0.1\%$. After the agglomeration, 1 mL of LA solution in the respective electrolyte was added so that the final concentration of LA in solution was 0.1 wt% or 11.1 mmol, and the total volume of the solution was 75 mL. Samples were withdrawn for analysis immediately after addition of LA and at intervals during the electrohydrogenation.

2.3. Analysis of products

Reaction mixtures were filtered using Millipore syringe filters (0.25 μm) to remove the catalyst and then analyzed by

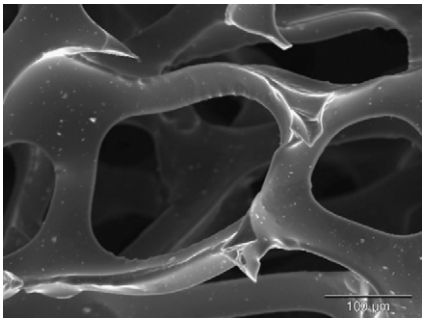

(a)

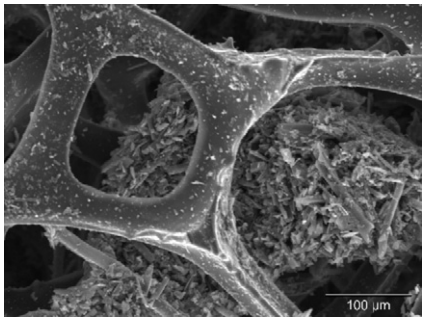

(b)

Fig. 2. SEM of RVC working electrode (100 ppi): (a) bare RVC electrode, (b) RVC electrode after entrapment of Ru/C via agglomeration for 2 h at 20 mA under cathodic polarization.

HPLC with refractive index detection, using a Biorad HPX87H ion exchange column at 65 °C. The mobile phase was 5 mmol H_2SO_4, run isocratically at a flow rate of 0.6 mL/min.

2.4. In situ ATR-FTIR

The sample cell consisted of a hemispherical Si window (25 mm diameter) and a Teflon holder, screwed onto a stainless steel base plate. The glass ATR cell (about 20 mL in volume) was mounted on the base plate and sealed with an o-ring to prevent leaks. The surface area of the internal reflection element

(IRE) exposed to the solution was 3.14 cm^2. The cell consisted of a water jacket through which water was circulated to maintain a constant temperature. The counter electrode was a Pt wire, which was attached to the cell, and the Ag/AgCl reference electrode was connected through the salt bridge. The Si window, coated with a thin film of Ru on Au, was used as the working electrode. Electrical contact with the window was attained through a gold wire sealed to a Teflon holder, which was mounted in a glass tube. The gold wire was sealed to the glass tube at the top and the entire assembly was screwed onto the cell. A constant potential was applied using a PAR 173 potentiostat. Before the ECH experiments, an Au film was chemically deposited on the Si IRE using the method described by Osawa and co-workers [13]. Once the Au film was formed, the window was rinsed with milli-Q water and then immersed in a solution of 1 mmol $RuCl_3 \cdot xH_2O$ to deposit an adlayer of Ru^{3+} on the Au surface. The electroreduction of Ru^{3+} to Ru^0 was carried out in the spectroelectrochemical cell by applying a potential of 0.0 mV (vs Ag/AgCl).

After the cell was assembled, the water circulator was turned on. Once the temperature was stabilized at 30 °C, about 19 mL of water was added to the cell, and an IR spectrum was recorded. Then the required amount of electrolyte was added to the water so that the final electrolyte concentration was about 0.01 M. Argon gas was bubbled through the solution for about 30 min to remove oxygen and other dissolved gases. A constant potential of 0.0 V (vs Ag/AgCl) was applied for 10 min to reduce the Ru^{3+} adlayer to metallic Ru. The working electrode was then polarized at −400 mV, and an IR spectrum was recorded. Then the required amount of LA solution was added so that the final concentration of LA in the system was 0.01 M and this point marked the beginning of ECH. The working electrode was maintained at a constant potential of −400 mV, and IR spectra were recorded every 8 min for 20 h.

FTIR spectra were taken with a Nicolet 20SX/C FTIR spectrometer, equipped with a liquid nitrogen-cooled linearized narrow band MCT-B detector. The sample compartment was purged using CO_2 and H_2O free air from a Puregas heatless dryer. The source (Everglow) was focused at the electrode/electrolyte interface by passing it through the Si window. The incident angle was 30° from the surface normal, the beam diameter was 8 mm, and the area of the IRE exposed to the solution was 3.14 cm^2. Each spectrum was acquired by integrating 1000 interferograms with a resolution of 4 cm^{-1}, to achieve the required sensitivity. The acquisition time was 8 min per spectrum. All spectra are shown in absorbance units, defined as $A = -\log(I/I_0)$, where I and I_0 are the intensities of the reflected radiation at the sample and reference solutions, respectively.

Table 1
Yields of products of ECH of lactic acid at various temperatures in 0.01 M H_2SO_4 after 9 h; current = 40 mA

Temperature (°C)	LA remaining (%)	LAL (%)	PG (%)	Material balance (%)
25	71.8	1.2	1.6	74.6
50	63.0	3.3	3.5	69.8
70	66.3	4.2	5.1	75.6
90	67.0	5.7	9.8	82.5

2.5. Ab initio calculations

Heats of formation were calculated from atomization enthalpies using the G3 composite ab initio method [14] as implemented in the Gaussian 98 code [15]. A 32-processor SGI Origin 3400 supercomputer was used for all of the calculations. The energetic consequences of solvation in water were approximated using the polarized continuum model (CPCM), calculated at the B3LYP/6-311 + G(d,p)//MP2/6-31G* level [16].

3. Results and discussion

As summarized in Tables 1 and 2 and in Scheme 2, ECH of LA yields LAL and/or PG under all conditions studied. The reaction's electrical efficiency was found to be highly dependent on the nature of the cell and the stability and dynamics of the system. The reductive catalyst agglomeration procedure before substrate addition was used to ensure that all Ru in contact with the RVC was in the metallic state and saturated with hydrogen. This step is equivalent to catalyst reduction in traditional batch hydrogenation.

The present ECH studies were carried out with 5% Ru/C/RVC to allow us to compare the results with the previously reported chemical hydrogenation of LA [1], because this catalyst was found to give the maximum rate of hydrogenation in

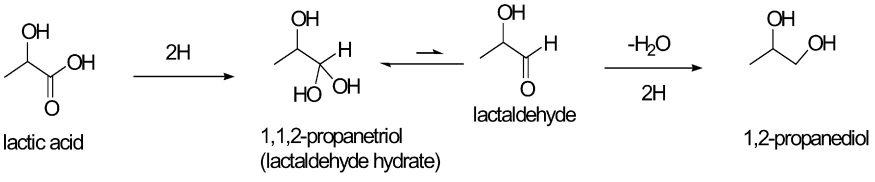

	lactic acid	1,1,2-propanetriol (lactaldehyde hydrate)	lactaldehyde	1,2-propanediol
Gas phase	-147.9	-151.5	-142.8	-161.0
Liq. phase	-158.8	-163.5	-156.7	-177.3

Scheme 2. Lactic acid hydrogenation reaction along with the results of the ab initio calculations of heats of formation (kcal/mol). Total heats of formation listed include implicit H_2 ($\Delta H_f = 0$) and H_2O (ΔH_f(gas) = −57.8 kcal/mol; ΔH_f(liq) = −68.3 kcal/mol) reactants and byproducts along with the species explicitly shown.

Table 2
Final yields (%) of products after lactic acid (11.1 mM) electrohydrogenation in various electrolytes; current = 100 mA, temperature = 70 °C

Electrolyte	Lactic acid (% remaining)	Lactaldehyde	1,2-propanediol	Material balance	Current efficiency
	Time = 48 h				
0.1 M H_2SO_4	91.8	2.6	2.7	97.1	7.48×10^{-7}
0.1 M HCl	8.9	64.0	6.6	79.5	7.17×10^{-6}
0.1 M $HClO_4$	54.5	25.4	0.7	80.6	2.48×10^{-6}
	Time = 21 h				
0.01 M H_2SO_4	37.4	29.1	4.5	71.0	8.09×10^{-6}
0.01 M HCl	9.4	80.3	2.9	92.6	1.83×10^{-5}
0.01 M $HClO_4$	0.2	58.6	1.1	59.9	1.29×10^{-5}

those studies. The same factors that lead to the high rate in the chemical hydrogenation—namely the stabilization of surface bound intermediates, electronic properties and particle size of the metal, structure and properties of the support and extent of adsorption of various species on the metal and support—would also be expected to favor the ECH process.

This choice drew on our early attempts at ECH of LA using Ru/carbon felt and 10% Ru/Pt mesh electrode in 0.01 M H_2SO_4 under similar conditions. These efforts produced only LAL and in much lower yields compared with the current work; formation of PG was seen only when the electrohydrogenation was carried out using 5% Ru/C catalyst agglomerated in the RVC working electrode. Evidently, the hydrogenation of LA to PG depends on specific characteristics of the Ru/C catalyst, such as the nature and distribution of pores and of the Ru nanoparticles in these pores. This notion was confirmed by similar experiments with 5% Ru/SiO_2 and 5% Ru/$BaSO_4$ particles suffused into the RVC. Here the catalyst supports were of lower porosity compared with carbon, and the Ru particles were larger and distributed mainly on the outer surface. In both cases, LAL was the only ECH product.

To maximize current efficiency, ECH should be carried out under conditions that minimize the competing hydrogen evolution by the Tafel or Heyrovski processes [3,4]. Beyond the control experiments below, reaction optimization studies were carried out to explore the effects of temperature, current, and electrolyte identity and concentration.

3.1. Control experiments

A control experiment carried out at 90 °C using the RVC with no catalyst in 0.01 M H_2SO_4 showed no LA conversion. Thus, the RVC alone is incapable of hydrogenation. Another control with Ru/C catalyst and gaseous hydrogen (1 atm) run at 90 °C in the absence of the RVC similarly showed no reaction, confirming that Ru needs to be in electrical contact for hydrogenation of LA to occur at the mild conditions of this study.

To confirm the unexpected formation of LAL via ECH of LA, glycolic (2-hydroxyacetic) acid, the C_2 analogue of lactic, was subjected to electrohydrogenation in 0.01 mol $HClO_4$ at 70 °C and 100 mA current for 21 h. The products of electrohydrogenation were analyzed by HPLC-RI, ESI-MS, and ^{1}H NMR. Almost complete conversion of glycolic acid to glycolic aldehyde was observed. Similarly, glyceric acid and alanine were converted to glyceraldehyde and 2-amino propanal, respectively. All of these products are well known, and their identification and quantification is straightforward.

As an additional control experiment, LAL, synthesized chemically using the procedure described by Nambiar et al. [17], was subjected to electrohydrogenation in 0.01 M $HClO_4$ at 70 °C and 100 mA current. There was negligible conversion of LAL to PG. LAL produced in situ from pyruvaldehyde dimethyl acetal and from pyruvaldehyde was also not significantly hydrogenated to PG.

3.2. Effect of temperature

Electrohydrogenation experiments with 11.1 mM LA in 0.01 M H_2SO_4 were carried out at 25, 50, 70, and 90 °C for 9 h using a constant current of 40 mA. The temperatures used span the practical temperature window for an aqueous electrolyte at atmospheric pressure, and they approach the lowest temperature (90 °C) at which conversion was observed in the chemical hydrogenation of LA.

With rising temperature, yields of LAL and PG increased (see Table 1) indicating increasing current efficiency. At higher temperatures, both ECH and hydrogen desorption by the Tafel reaction accelerate; the ECH relative rate increase, however, suggests that ECH competes more effectively for surface H atoms at higher temperatures. Relative rates of hydrogenation and hydrogen evolution are thought to depend on the intrinsic thermochemistry of the reduction, adsorption modes and energies of the reactants and products, and the activity of chemisorbed hydrogen [4a]. Similar increases in the conversion and current efficiency with increasing temperature have been previously noted in the ECH of (a) lignin models such as guaiacol [9] and 4-phenoxy phenol [10] to phenol and cyclohexanol over Raney Ni powder and 5% Pd/C in an RVC electrode using 1 mol NaOH as the electrolyte, where Menard et al. found a slight increase in conversions with increase in the temperature from 25 to 50 °C; (b) 4-amino-5-nitrosodimethyl uracil on a foamed nickel cathode in $(NH_4)_2SO_4$ solution, studied by Hu et al. [18]; (c) phenol to cyclohexanol on dispersed Pt electrode in 0.05 mol H_2SO_4, studied by Amouzegar and Savadogo [19]. Interestingly, in the ECH of vat dyes such as indigo in 1 mol NaOH, Roessler et al. [20] observed an increase in conversion up to 60–80 °C, but current efficiency and conversion then dropped off above this temperature; these findings were interpreted in terms of the competition between hydrogen incorporation into the substrate and decreasing surface concentration due to H_2 desorption. Bryan and Grimshaw [21] found that efficiency increased with temperature without changing the C=C versus C=O product selectivity in the ECH of 4-phenylbutene-2-one to 4-phenylbutan-2-one on a Ni cathode in ethanol containing H_2SO_4. In all of these cases, the reported trends were believed to be due to greater increase in the rate of hydrogenation compared with hydrogen evolution.

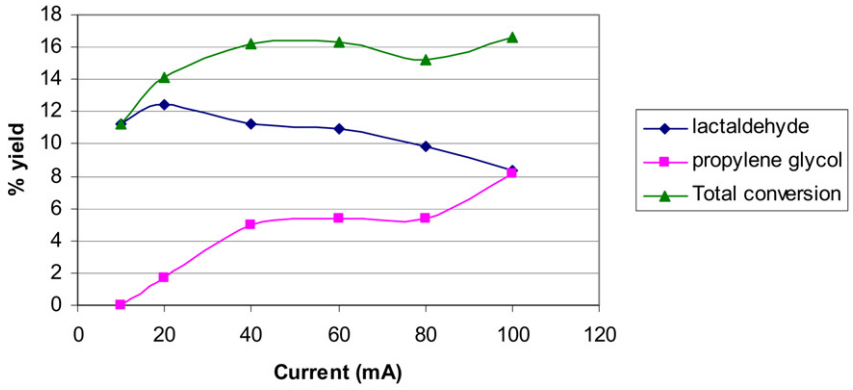

Fig. 3. Yield of lactic acid reduction products after electrohydrogenation in 0.01 M H_2SO_4 for 9 h at 90 °C. Only lactaldehyde and propylene glycol were detected; "total conversion" refers to the sum of these products.

3.3. *Effect of current*

Electrohydrogenation of 11.1 mM LA in 0.01 M H_2SO_4 for 9 h at 90 °C at different currents indicated that with increasing current, the yield of PG increases and that of LAL decreases slightly, as shown in Fig. 3. Like Polcaro et al. [7] in their studies of benzaldehyde and acetophenone reduction, we assume that the density of surface H atoms increases with increasing current, as does reaction of LA, but the competing Tafel reaction (second order in H atoms) accelerates more. Viewed this way, the fact that the current efficiency of LA reduction is maximal at 10 mA suggests only a need for isolated hydrogen atoms. On the other hand, the conversion of LA to PG at low current (10 mA) is close to zero and rises with increasing current, in spite of the attendant increased rate of hydrogen evolution. Assuming the sequential mechanism of Scheme 2, the aldehyde reduction step appears to require adsorbed molecular hydrogen (or at least closely spaced atoms) on the surface. Although one might hope that the kinetic studies of classical hydrogenation would allow a distinction to be made between surface-bound H_2 molecules and H atoms, models invoking both situations have been successful at modeling the kinetic behaviors of LA and the closely analogous alanine reductions [1,2].

In the ECH of cyclohexenone using a nickel boride electrode, Mahdavi et al. [6] observed a decrease in the conversion efficiency with increasing current density due to a relatively greater increase in the rate of hydrogen evolution compared with hydrogenation. However, there was an increase in the further hydrogenation of cyclohexanone to cyclohexanol. This was explained by the idea that the more negative potential at higher current densities would activate the chemisorbed hydrogen for faster hydrogenation of the cyclohexanone molecules generated at the electrode surface by cyclohexenone hydrogenation. Cyclohexanone is expected to be more weakly adsorbed on the electrode surface compared with the conjugated enone, cyclohexenone. At lower current densities, cyclohexanone hydrogenation would be too slow to compete with desorption and diffusion to the bulk solution. On the other hand, Senda et al. [22] saw an increase in ECH of 4-*t*-butylcyclohexanone to alcohol with decreasing current.

The case of LA hydrogenation appears similar to the aforementioned findings of Mahdavi et al., but more complex due to the intermediate dehydration step involved before LAL can be further hydrogenated to PG (Scheme 2). With increasing currents, yields of LAL and PG decrease and increase, respectively, while the total conversion remains almost constant. As shown in Scheme 2, the simplest interpretation is that LA conversion to PG occurs via two sequential hydrogen additions with LAL hydrate and LAL as discrete intermediates. At low current, displacement of the relatively weakly bound LAL hydrate (1,1,2-propanetriol) by LA is faster than its dehydration and capture by surface hydrogens. At higher currents LAL (also relatively weakly bound) would be more quickly converted to PG due to the availability of more surface hydrogen atoms. But the nearly complete absence of PG at low currents suggests another factor: base-promoted acceleration of LAL formation at the surface via dehydration of LAL hydrate in the diffusion layer. Like other carbonyl hydrates, LAL hydrate's equilibration with the free carbonyl form is accelerated at pH values both above and below neutral [23]. At higher currents, solution protons are more quickly adsorbed and reduced, so the pH at the cathode surface is also higher. Not only are more hydrogen atoms available for reaction, but also the concentration of free LAL in proximity to the surface is enhanced, increasing PG formation.

The increase in the rate of formation of PG at higher current may also be favored by the higher electrode surface energy at more negative potential, resulting in higher mobility of H atoms, similar to the phenomenon observed by Mahdavi et al. [6] in the ECH of cyclohexenone. The trend observed here also points to the involvement of overpotential deposited hydrogen (OPD-H), rather than underpotential deposited hydrogen (UPD-H) in the ECH of LA. UPD-H atoms are strongly bound to the electrode surface and are believed to be formed on Ru at around 0.0 V, whereas the weakly bound OPD-H atoms are formed at more negative potentials and may coexist with UPD-H. These weakly bound H atoms were found to be involved in the hydrogen evolution reaction [44] and in the ECH of the olefinic double bond in substrates such as maleic acid [24].

An alternative to the sequential interpretation of Scheme 2 involves independent paths: parallel reactions might form LAL

and PG simultaneously from LA adsorbed on two different types of catalytic sites. In the ECH of benzaldehyde and acetophenone by Polcaro et al. [7], the aldehydes were converted to two different products, the corresponding alcohol and hydrocarbon; the formation of the two types of products were assumed to involve parallel reactions of the aldehyde adsorbed on different catalytic sites. Adsorption of aldehyde on low coordination sites such as steps and kinks was assumed to lead to the formation of hydrocarbon whereas the alcohol was thought to form by adsorption on high co-ordination sites. Consistent with this key role for catalyst structural features (e.g., terraces, step edges and kinks), the ratio of the two types of products were found to depend on catalyst particle size, morphology and method of preparation. Lacking information on the reactivity of multiple catalyst morphologies, we cannot rule out this two-site interpretation of the LAL and PG production. However, the sequential scheme is simple, consistent with all observations, and serves as the working model for this discussion.

3.4. Effect of electrolyte

Electrohydrogenation of 11.1 mmol LA was carried out in various electrolytes at 70 °C and 100 mA current. Electrolytes studied were H_2SO_4, $HClO_4$, and HCl at concentrations of 0.01 and 0.1 M. Although the ECH rate was maximal at 90 °C, the 70 °C temperature was chosen to prevent excessive water evaporation from the system during the long run times. The experiments with 0.01 M electrolyte could run only for 21 h because of the system's increasing resistance as protons were depleted.

The results, summarized in Figs. 4a and 4b, show considerable variation in the rates of LAL and PG formation in different electrolytes due to differences in the anions' reactivity and catalyst surface adsorption. The final yields of the products and current efficiencies are listed in Table 2. The low material balances may be due to sequestration of products in the catalyst's activated carbon support. Alternatively, losses to volatiles are possible; formation of volatile products such as methane have been seen in the more severe chemical hydrogenations of carboxylic acids with 5% Ru/C.

In general, in both 0.1 and 0.01 M electrolyte concentrations, the rate of formation of LAL was found to decrease in the order $HCl > HClO_4 > H_2SO_4$. Formation of PG was generally slow, maximal in 0.1 M HCl and almost negligible in 0.1 M $HClO_4$ due to an inhibitory effect of the ClO_4^- anion. In the case of ECH of LA in 0.01 and 0.1 mol HCl, the rate of conversion of LA to LAL and PG was low initially and increased over time. Apparently, as the electrohydrogenation proceeds, Cl_2 evolution at the anode decreases the Cl^- concentration in solution, leading to the desorption of Cl^- from the cathode surface and leaving more sites for the adsorption of LA, hydrogen, or other active species. It is also possible that partial surface coverage by adsorbed Cl is beneficial for the ECH reaction, because the electronegative Cl atoms modify the electronic state of the Ru atoms and enhance adsorption of reactants. To test this hypothesis, ECH of LA was performed in the absence of an electrolyte. With a pK_a of 3.86, LA at 11.1 mmol is expected to be largely ionized and thus able to function as the electrolyte. The solution's resistance was high, however, limiting the practical ECH current to half the usual value (i.e., 50 mA). Nonetheless, at this current, the quantity of H atoms produced should be sufficient to completely hydrogenate all of the LA present in solution. As expected, no PG formation was observed in this case; presumably, the low solution concentration of protons could not provide the high surface coverage of H needed for PG formation. Importantly, there was no induction period, a finding that supports the Cl adsorption explanation for the initial low ECH in HCl electrolyte. However, the rate of ECH at later stages in the reaction was not as high as that seen with HCl; presumably, once Cl has desorbed, the relative ECH rates reflect the differences in current (50 vs 100 mA) between experiments with LA alone and in the HCl electrolyte. The anomalous behavior observed with HCl may also reflect an electronic enhancement or surface restructuring effect of Cl on the Ru electrode surface, but the present results cannot make that determination.

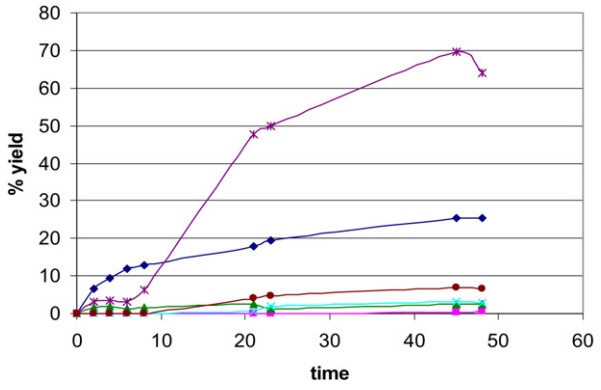

(a)

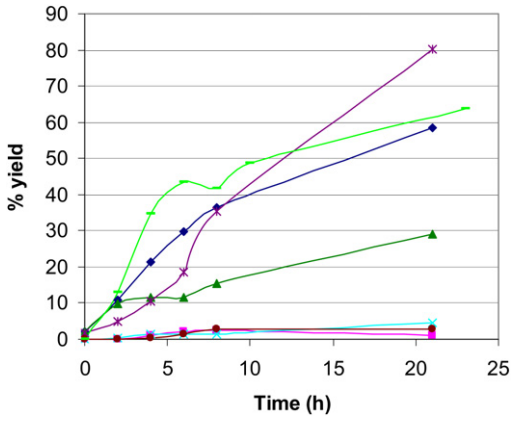

(b)

Fig. 4. Time course of product formation from electrohydrogenation of lactic acid in various electrolytes (0.1 M) at 70 °C. (a) (♦) Lactaldehyde (0.1 M $HClO_4$); (■) 1,2-propanediol (0.1 M $HClO_4$); (▲) lactaldehyde (0.1 M H_2SO_4); (X) 1,2-propanediol (0.1 M H_2SO_4); (∗) lactaldehyde (0.1 M HCl); (●) 1,2-propanediol (0.1 M HCl). (b) (♦) Lactaldehyde (0.01 M $HClO_4$); (■) 1,2-propanediol (0.01 M $HClO_4$); (▲) lactaldehyde (0.01 M H_2SO_4); (X) 1,2-propanediol (0.01 M H_2SO_4); (∗) lactaldehyde (0.01 M HCl); (●) 1,2-propanediol (0.01 M HCl); (—) lactaldehyde (no electrolyte).

The adsorption of anions on electrode surfaces and their effects on hydrogen adsorption on metal surfaces have been extensively studied. The relative strengths of adsorption of the

anions were found by Horanyi to decrease in the order $Cl^- > HSO_4^- > ClO_4^-$ on Pt electrode [25]. In studies of chemical catalytic hydrogenation of LA, Cl^- was found to significantly inhibit hydrogenation, whereas the inhibitory effect was observed only in the early stages in ECH. This discrepancy reflects the fundamental difference in the initial step of the two processes. In catalytic hydrogenation, the first step in the process is the dissociation of the H_2 molecule into atoms, which is equivalent to the electrocatalytic oxidation of H_2. In the case of ECH, the initial step involves the cathodic reduction of protons in solution. Adsorption of anions was found to inhibit the hydrogen oxidation process on Pt, but not the electroreduction step [24]. Therefore, the effect of anions depends on the source of H atoms (i.e., molecular H_2 or protons). This difference was attributed to the involvement of overpotential deposited (OPD) H atoms in ECH and not underpotential deposited (UPD) H atoms, the adsorption of which is influenced by anion adsorption. OPD hydrogen atoms are weakly bound on the cathode surface and have a certain degree of mobility, thus enabling them to reach the active sites. However, in the case of ECH of LA on Ru, the adsorption of anions seem to be strong and accompanied by some amount of charge transfer because they are not easily desorbed even in the hydrogen evolution region. The increase in ECH activity at more negative potentials also may be attributed to the increased mobility of OPD H atoms and a change in the electronic properties of the metal surface due to cathodic polarization [24]. Several studies found that the adsorption of Cl^- on the electrode surface shifted the metal oxide formation peak in the cyclic voltammogram to more positive potentials and the hydrogen adsorption peak to more negative potentials [26]. Therefore, Cl^- adsorption was found to inhibit the formation of metal oxides such as RuOH, resulting in increased hydrogen adsorption. Some Cl^- adsorption was assumed to occur even at more negative potentials of hydrogen evolution. Therefore, the enhancing effect of HCl toward ECH of LA observed in our studies may be attributed to the inhibition of Ru oxide formation. The adsorption of Cl^- does inhibit LA conversion initially, but the effect is overcome at longer times by the desorption of Cl^- resulting from anodic oxidation of Cl^- and reduced solution concentration.

FTIR spectroscopy has shown that HSO_4^- and ClO_4^- adsorb on metals through three of the O atoms in a C_{3v} configuration [27–29]. Even though ClO_4^- is considered weakly adsorbed on electrode surfaces in many cases, Colom and Gonzalez-Tejera [30] observed electroreduction of ClO_4^- to Cl^- on Ru electrodes. The extent of reduction was found to depend on the concentration of ClO_4^-, hydrogen adsorption, and temperature. Perchlorate reduction process requires the presence of adsorbed hydrogen and is enhanced at higher temperatures. Therefore, despite the similar modes of adsorption of the anions, the enhancement of LAL formation with perchlorate may be attributed to some extent to its decomposition to Cl^- on the surface, followed by the desorption and anodic oxidation of Cl^-. Cl_2 gas evolution at the anode was observed when $HClO_4$ was used as the electrolyte. However, it is interesting to note that there is significant concentration-dependent inhibition of LAL and PG formation with 0.01 and 0.1 M H_2SO_4 and $HClO_4$.

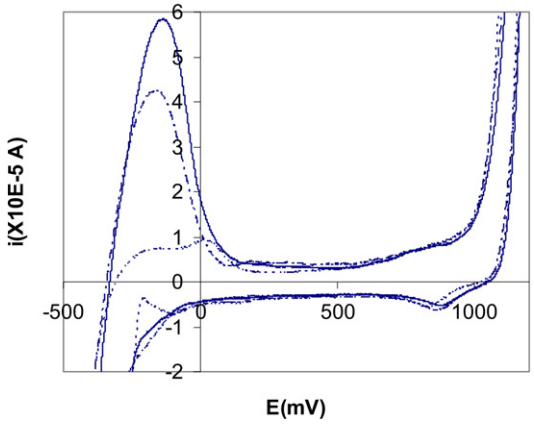

(a)

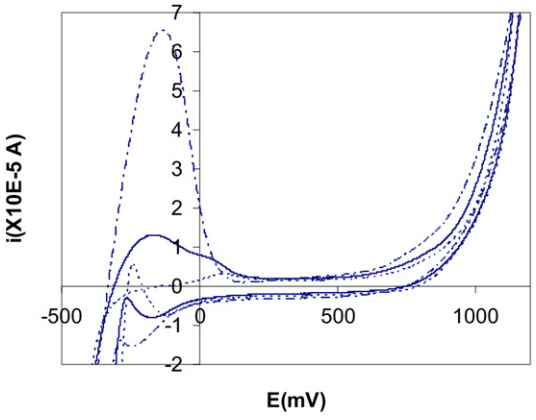

(b)

Fig. 5. Cyclic voltammogram of Ru polycrystalline electrode in various electrolytes (0.01 M) ($A = 0.2\ cm^2$, $\upsilon = 10$ mV/s): (a) without lactic acid and (b) in the presence of lactic acid (0.01 M). (—) $HClO_4$, (- - -) H_2SO_4 and (-·-·-) HCl.

Comparison of rates of product formation between the various electrolytes reveals that SO_4^{2-} has a significant detrimental effect toward LAL formation, whereas perchlorate significantly inhibits PG formation at only high concentration. These results indicate a general adsorption of Cl^- on all types of active sites, whereas perchlorate and sulfate show preferential adsorption on specific active sites. On the basis of in situ FTIR studies, Marinkovic et al. [31] reported that due to a near-ideal geometrical fit to the Ru lattice's dimensions and hexagonal symmetry, bisulfate ions adsorb strongly on Ru(0001) surface at potentials about 300 mV more negative than for adsorption on Pt, whereas their adsorption on polycrystalline Ru is inhibited by surface oxide formation. The potential at which anion adsorption on a metal surface occurs is determined by its work function [32].

3.5. Voltammetric studies

Figs. 5a and 5b show cyclic voltammograms of polycrystalline Ru electrode (0.2 cm^2) in the three electrolytes at 0.01 M concentration in the absence and presence of LA (11.1 mM) recorded at a scan rate of 10 mV/s. In all cases, the cathodic hydrogen adsorption and anodic hydrogen oxidation/desorption peaks can be observed. In Fig. 5a, in $HClO_4$ and HCl, the H adsorption peaks overlap with the hydrogen evolution cur-

rent. In addition, oxygen evolution occurs at much lower potentials in the presence of LA. However, in case of H_2SO_4, there is significant hysteresis in both the absence and presence of LA, which can be attributed to the difference in the properties of the surface caused by anion adsorption on Ru [33]. The peak currents are also much lower in H_2SO_4. Unlike $HClO_4$ and HCl, there is a delay in the onset of hydrogen desorption in H_2SO_4, indicating the formation of a stable adlayer of H which is resistant to oxidation. All of these results are consistent with adsorption of sulfate on Ru at the H adsorption/desorption potential. There is no cathodic peak after the hydrogen desorption peak during the positive sweep in 0.01 M $HClO_4$, indicating that perchlorate reduction to chloride, which is known to be a slow and irreversible process at room temperature [27], does not occur at this scan rate and at this concentration.

In the presence of LA (Fig. 5b), the hydrogen adsorption peak currents decrease in the case of H_2SO_4 and $HClO_4$ due to partial blocking of surface sites by LA adsorption, but remain constant in the case of HCl. This indicates that in HCl, in spite of LA adsorption, the surface coverage of adsorbed hydrogen remains constant due to an enhancement of hydrogen adsorption by adsorbed Cl. Using radiotracer analysis, Horanyi and Rizmayer [34] reported strong adsorption of Cl on Ru in the hydrogen adsorption/evolution region at negative potentials even with high surface coverage of H and stated the possibility of Cl^- ions influencing the adsorption of H and O on Ru. They also showed much stronger adsorption of Cl^- ions compared with ClO_4^- and SO_4^{2-}. The cyclic voltammograms yield some information about the extent of anion adsorption in the hydrogen adsorption region, but not in the more negative hydrogen evolution region, where ECH actually occurs. ATR-SEIRAS studies of the ECH of LA, described in the subsequent section gives more detailed information about the effect of anion adsorption on ECH.

3.6. *In situ ATR-FTIR studies of ECH of LA*

The IR spectra of LA recorded at various times at 30 °C and −400 mV in the three electrolytes H_2SO_4, HCl, and $HClO_4$, using the spectra recorded after 1200 min as the reference, are shown in Figs. 6a, 7a and 8a. The O–H stretching and H–O–H bending regions are shown separately in Figs. 6b, 7b and 8b. These spectra were referenced against the spectra of the respective electrolytes alone taken under identical conditions, to clearly see the changes occurring during ECH of LA without significant interference from solution LA. The spectra below 1200 cm^{-1} are not shown in the figures because the cutoff frequency for the Si window is 1200 cm^{-1}. The LA concentration used in all cases was 0.01 M, which was the concentration calculated to give minimum interference from solution phase LA. The peak positions and assignments of the initial spectrum in each case, taken immediately after addition of LA to the electrolyte are shown in Table 3. The spectra clearly show strong bands due to the COO symmetric stretch and the alcoholic C–O stretch, indicating that LA is adsorbed on Ru in the chelating bidentate mode. Therefore, the α-hydroxy group is not involved

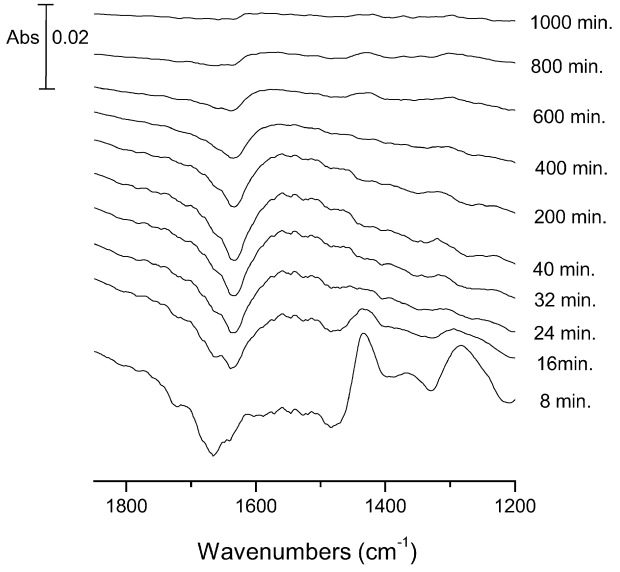

(a)

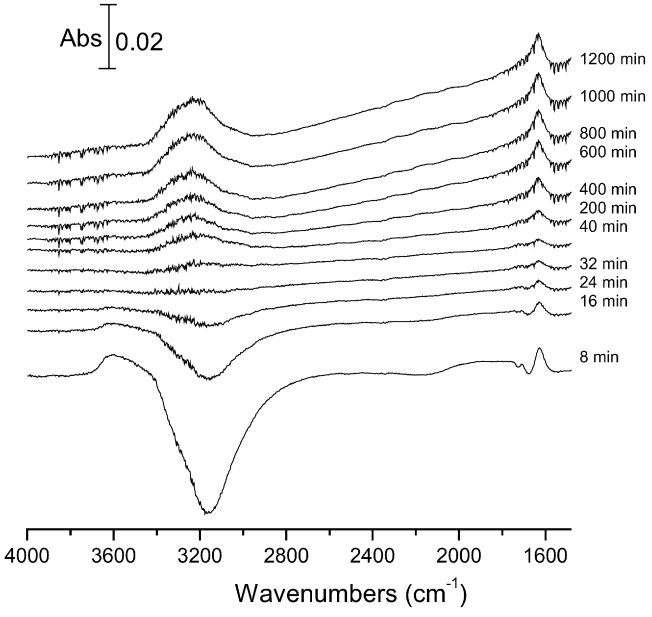

(b)

Fig. 6. Real time ATR-IR spectra of the ECH of lactic acid in 0.01 M H_2SO_4 ($T = 30$ °C, $E = -400$ mV) (a) using the spectrum taken after 1200 min as the reference, and (b) using the spectrum of 0.01 M H_2SO_4 taken under identical conditions as the reference, showing the O–H stretch and H–O–H bending bands.

in bonding to the metal catalyst. The weak or negative bands observed around 1710 cm^{-1} may be attributed to the C=O stretch of solution phase LA. The monodentate and the dissociative adsorption modes may be ruled out as these modes would result in much stronger C=O stretching bands.

The spectra show strong symmetric stretching (1435 cm^{-1}) and weak asymmetric stretching bands. These observations can be explained by the surface selection rule [35] and strongly support the chelating bidentate mode of adsorption and the fact that spectra show predominantly adsorbed LA species, because SEIRAS is sensitive to surface species and less sensitive to

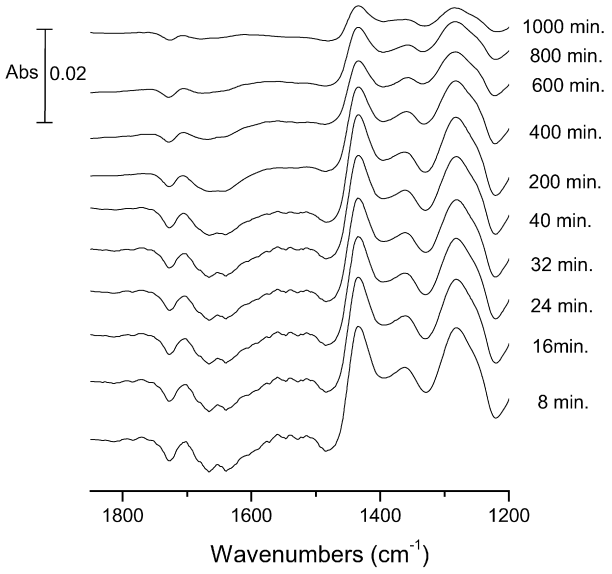

(a)

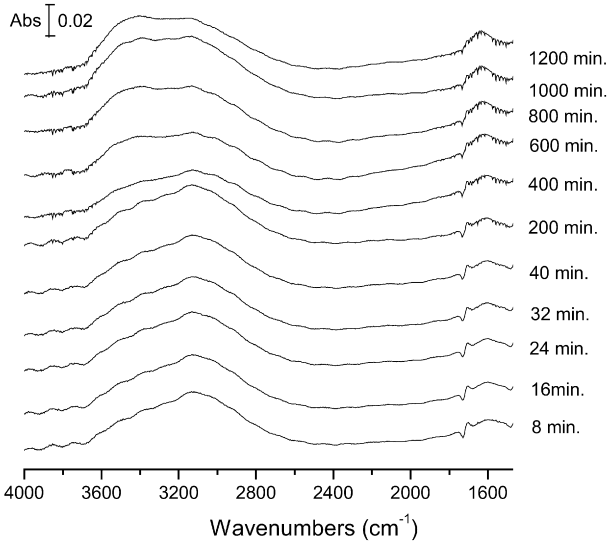

(b)

Fig. 7. Real time ATR-IR spectra of the ECH of lactic acid in 0.01 M HCl ($T = 30\,^{\circ}C$, $E = -400$ mV) (a) using the spectrum taken after 1200 min as the reference, and (b) using the spectrum of 0.01 M HCl taken under identical conditions as the reference, showing the O–H stretch and H–O–H bending bands.

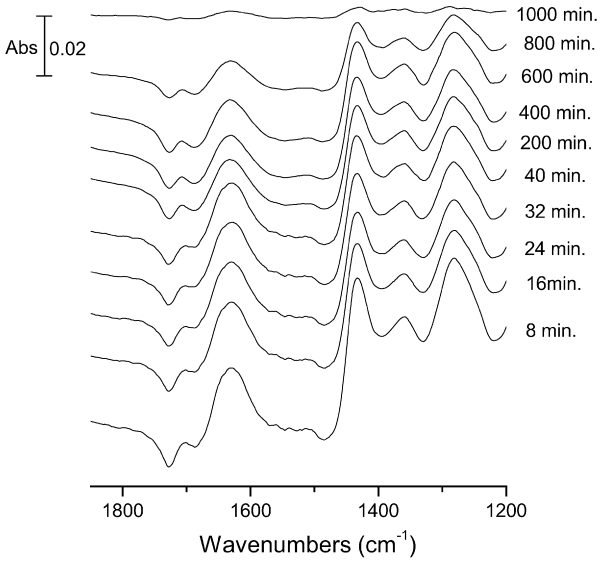

(a)

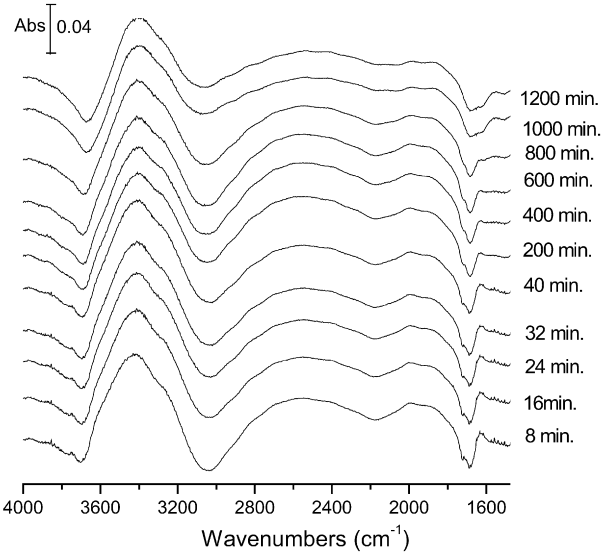

(b)

Fig. 8. Real time ATR-IR spectra of the ECH of lactic acid in 0.01 M $HClO_4$ ($T = 30\,^{\circ}C$, $E = -400$ mV) (a) using the spectrum taken after 1200 min as the reference, and (b) using the spectrum of 0.01 M $HClO_4$ taken under identical conditions as the reference, showing the O–H stretch and H–O–H bending bands.

solution species. The transition dipole of the symmetric COO vibration is parallel to the diagonal of the carboxylate group and when LA is coordinated to the metal surface through the carboxylate group has a strong component in the direction normal to the surface, which explains the high intensity of this band. In contrast, the direction of transition dipole of the COO asymmetric stretch is along the line joining the two oxygen atoms, which in the adsorbed molecule is parallel to the surface and hence this vibration is IR inactive. The O–H deformation mode also gives a weak band at 1357 cm^{-1} due to this bond being parallel to the surface when LA is adsorbed in the chelating bidentate orientation.

In 0.01 M H_2SO_4 (Fig. 6a), as the reaction progresses, several changes are observed in the spectra. The peak at 3168 cm^{-1} due to the O–H stretching vibration of strongly hydrogen bonded water reappears and the peaks at 1435 and 1283 cm^{-1} from adsorbed LA decrease in intensity. This indicates that as the reaction progresses, the Ru surface is poisoned and this results in a decrease in the adsorption of LA. The poison may be associated with reaction intermediates, sulfate or S-containing species derived from the sulfate ions of the electrolyte, because the decrease in LA adsorption is associated with the appearance of strongly hydrogen bonded water near the electrode surface, which are known to be associated with the hydrophilic sulfate anions, from previous studies of interfacial water molecules on

Table 3
IR peak assignments for the initial spectrum taken at 8 min during ECH of lactic acid

Wave number (cm^{-1})	Vibrational mode
0.01 M H_2SO_4	
1283	υC–O (α-hydroxy)
1357	O–H deformation
1435	υCOO symmetric
1630	δH–O–H
3610	υO–H (water and lactic acid)
0.01 M HCl	
1283	υC–O (α-hydroxy)
1357	O–H deformation
1435	υCOO symmetric
1595	δH–O–H
3120	υO–H (water and lactic acid)
0.01 M $HClO_4$	
1275	υC–O (α-hydroxy)
1340	O–H deformation
1435	υCOO symmetric
1625	δH–O–H
3400	υO–H (water and lactic acid)

Au electrode by Osawa and co-workers [36,37]. This poisoning effect explains the lower rate of ECH of LA in H_2SO_4 compared with HCl and $HClO_4$.

In 0.01 mol H_2SO_4 (Fig. 6b), the negative band at 3168 cm^{-1} indicates the displacement of strongly hydrogen-bonded water molecules from the surface by LA. However, the bands at 1630 and 3610 cm^{-1} are due to the H–O–H bending and O–H stretching vibrations of non-hydrogen-bonded water molecules. Apparently, adsorption of LA on the electrode surface isolates bound water molecules, and such non-hydrogen-bonded water molecules show O–H stretching frequencies around 3600 cm^{-1} [38]. The shift in the O–H stretch frequency from this value gives an estimate of the extent of hydrogen bonding. The H–O–H bending frequency of water adsorbed on Ru(001) surface in UHV has been reported to be in the range of 1560–1520 cm^{-1} [36,39]. A downward shift of the O–H stretch frequency and an upward shift of the δH–O–H mode are indicative of strongly hydrogen bonded water [36]. The O–H stretching vibrations of LA cannot be distinguished from those of water, and the peak is believed to overlap with the 3610-cm^{-1} peak from water. The close-packed monolayer of LA adsorbed on Ru through the carboxylate groups are also expected to have –O–H groups, which are isolated from one another and from water molecules in the vicinity, forming very few hydrogen bonds, thus giving the high-frequency band around 3610 cm^{-1}.

In 0.01 M HCl (Fig. 7b), the O–H stretching bands from water and LA and H–O–H bending bands from water appear at 3120 and 1595 cm^{-1}, respectively. Therefore, the LA may be associated with strongly hydrogen-bonded water. However, in this case, it is clear from Fig. 7a that there is no significant decrease in intensity with time of bands due to adsorbed LA. Apparently, the Ru surface is not poisoned by electrolyte anions in this case.

It is also interesting to note the appearance of new bands at 3400 and 1647 cm^{-1} at around 200 min in Fig. 7b, associated with O–H stretching and H–O–H bending vibrations of water. The appearance of these bands corresponds approximately to the increase in the rate of ECH of LA after a slower initial phase, observed while using HCl as the electrolyte with 5% Ru/C agglomerated in RVC. This suggests that the partial desorption of chloride, as a result of decrease in the solution concentration of chloride as Cl_2 gas is evolved at the anode, frees up sites, allowing the adsorption of water molecules, which are required for ECH. From the frequencies of the water bands, they appear to be relatively isolated or poorly hydrogen bonded, which may be a result of association with the surface and the hydrophobic nature of the co-adsorbed chloride, resulting in disruption of hydrogen bonding [40–42]. These observations are consistent with the conclusion that adsorbed water plays an important role in LA hydrogenation, derived from the experiments indicating a decrease in the rate of hydrogenation of LA in organic solvent/water mixtures [8]. From ab initio studies of water layer on Pt(111) and Rh(111) surfaces, Vassilev et al. [43] discovered that water molecules adsorbed on a metal surface have a slight metal-like conductivity resulting from mixing of local states of the oxygen atom with the electron bands of the metal substrate. The extent of mixing of the atomic states from oxygen and metal was found to depend on the orientation of the water molecules, the distance from the surface, and the polarization of the surface. Analysis of the electronic states indicated an electron charge transfer from the water molecules toward the surface, resulting in a reduction of the work function of the system. This phenomenon may be responsible for facilitating the electron transfer to protons or H_3O^+ to form H atoms, which are required for ECH. In the case of H_2SO_4 and HCl electrolytes, a weak feature due to H_3O^+ was observed in the IR spectra. However, the peak corresponding to the M–H bond, known to appear around 2100 cm^{-1} [44,45] was not observed in any of the spectra, indicating that either the surface concentration of adsorbed H is too low to be detected by IR or it is a very short-lived species, with lifetime much shorter than the time scale of the scans.

The cyclic voltammetry results described earlier indicate that adsorbed Cl on the electrode surface when HCl is used as the electrolyte favors H adsorption. Therefore, the enhanced ECH rate in HCl is probably a result of the electronic effects of both adsorbed chloride and water. The specific sites occupied by the water molecules and the exact configuration required for involvement in the hydrogenation rate enhancement remains unclear.

In 0.01 mol $HClO_4$ (Fig. 8), there is a slight decrease in the intensity of the adsorbed LA bands with time at 1000 min, indicating poisoning of the surface by perchlorate or chloride, but the decrease in intensity is not as pronounced as in the case of H_2SO_4 and occurs at much longer time compared with the H_2SO_4 case. The negative C=O stretching band in all the three electrolytes may be explained by the fact that some LA is still present in solution at the end of ECH (i.e., at 1200 min), and in the absence of significant amounts of adsorbed LA (due to electrode surface poisoning), show stronger IR bands in comparison to the spectra taken during the earlier stages of ECH.

Why does electrohydrogenation of LA stop at LAL, rather than progressing on to 1,2-propanediol as in the chemical reduction? The most likely reason is that the LA reduction leads directly to the hydrated form of LAL, as shown in Scheme 2. Like other α-hydroxy aldehydes, LAL strongly favors the hydrated form at equilibrium. Under the relatively low temperature and acidic conditions of ECH, the dehydration required to enable further hydrogenation to the diol would be slower than its desorption, thus leading to the formation of small quantities of PG. The formation of PG is also favored by higher surface concentration of H. This notion is also supported by the fact that when mandelic acid, an aromatic analog of LA, was subjected to ECH under similar conditions, the completely hydrogenated product cyclohexyl ethylene glycol was formed to an approximate 50% extent, much higher than the LA-to-PG conversion. The intermediate cyclohexyl glycolic aldehyde also present in the product mixture is expected to be less hydrated than LAL due to the greater electron-donating effect of the cyclohexyl substituent.

A similar selectivity to the corresponding aldehyde was observed by Yokoyama and Yamagata [46] in the vapor-phase hydrogenation of benzoic acid using Cr/ZrO_2. In this case, the carboxylic acid interacts strongly with the catalyst surface, displacing the weakly bound aldehyde as soon as it is formed, preventing successive hydrogenation to the alcohol and resulting in high aldehyde selectivity (96 at 98% conversion in the Yokoyama and Yamagata [46] case). Studies of LA, PG, and glycerol binding on Ru surfaces have shown stronger LA binding by at least 2 orders of magnitude. In terms of chemical functionality, the hydrated LAL (1,1,2-propanetriol) is much more like PG and glycerol than LA, and its expected affinity for the surface should be similarly weak [47]. Thus, like Yokoyama and Yamagata [46], we interpret the LAL preference as evidence for the desorption rate exceeding the dehydration/hydrogenation rate at these low temperatures. The results of the ab initio calculations of heats of formation shown in Scheme 2 indicate that the dehydration of hydrated LAL in the liquid phase is endothermic by 6.8 kcal/mol. However, the other two steps—hydrogenation of LA to hydrated LAL and the hydrogenation of LAL to PG—are exothermic, for an overall LA-to-PG exothermicity of 18.5 kcal/mol. Although gas-phase heats of formation calculated this way are typically within 1–2 kcal/mol of experimental values, the simulation of aqueous solution via continuum methods ignores specific hydrogen-bonding contributions; thus, these "solution" energy changes are based on the approximation that errors in representing such interactions are of similar magnitude for all species.

It is also interesting to note that although no LAL formation was observed in the Ru/C-catalyzed aqueous-phase chemical hydrogenation of LA, Dumesic and co-workers [48] did observe LAL formation in the vapor-phase hydrogenation of LA using 10% Cu/SiO_2 catalyst. The formation of the aldehyde was found to be dependent on the equilibrium between the aldehyde and diol at a given hydrogen partial pressure. The highest yield of LAL (22.2%) was obtained at a hydrogen partial pressure of 0.10 MPa at 473 K, and the yield was found to decrease with decreasing temperature and increasing hydrogen partial pressure. Acetaldehyde formation by the vapor-phase hydrogenation of acetic acid over silica-supported copper catalyst was also described by Cortright and Dumesic in an earlier report [49]. In these cases, aldehyde formation was attributed to the hydrogenation of intermediate surface acyl species. However, in the present work, dissociative adsorption of LA and consequent surface acyl formation can be ruled out from the FTIR results. Falorni et al. [50] reported the Pd/C catalyzed hydrogenation of substituted amino acids to aldehydes at atmospheric pressure in ethanol. The conversion involved the preparation of an ester with 2-chloro-4,6-dimethoxyl[1,3,5]triazine, followed by hydrogenation. Reduction of the aldehyde to alcohol was reported only at higher pressures and longer reaction times. However, as with our mandelide studies, alcohol was formed as the major product when aromatic carboxylic acids were used. These studies reflect a dependence of the relative rates of product formation on the surface hydrogen concentration, reaction conditions, and mode of adsorption of the substrate.

4. Conclusion

Electrocatalytic hydrogenation of LA has been accomplished using 5% Ru/C agglomerated in RVC under mild conditions of temperature and pressure compared with chemical catalytic hydrogenation. The major product of electrocatalytic hydrogenation was LAL, with small quantities of 1,2-propanediol. This unexpected process can provide a clean, convenient, and efficient method for preparing LAL, a compound that is not commercially available and is difficult to obtain in pure form. To the best of our knowledge, this is the first ECH study conducted on a carboxylic acid. The low current efficiency is due to the slow kinetics of the ECH reaction. In the 5% Ru/C/RVC system, the amount of active electrocatalyst at any given time is very low, because the technique relies on efficient agglomeration of the catalyst, which is affected by various factors, including particle size, fluid dynamics, and others. The kinetics can be improved by developing better electrode materials based on Ru and C, which will consist of well-dispersed Ru nanoparticles on solid-phase carbon of similar porosity.

In preparative and mechanistic studies [1,51] of the Ru/C-catalyzed hydrogenation of LA to 1,2-propanediol, LAL was proposed as an intermediate but was never isolated. Using electrohydrogenation, LAL is the primary LA conversion product, supporting its proposed intermediacy en route to 1,2-propanediol. Although this project was begun as a way to carry out LA-to-PG reduction under mild conditions, the discovery of a pathway that directly reduces aqueous carboxylic acid to aldehyde and then stops is substantially more interesting in terms of both fundamental chemistry and practical processes. The fact that the product ratio of ECH depends on the electrolyte used is also intriguing and can be exploited in future applications to control the selectivity of the reaction toward specific products by using specific electrolytes or a combination of electrolytes.

The ECH of LA on Ru electrode surface was studied in real time using ATR-SEIRAS spectroscopy. The conditions used for the SEIRAS studies were close to those used for bulk ECH studies, so that the spectra can be correlated with changes oc-

curring on or near the electrode surface during the course of the experiment. The differences in rate of ECH observed in the three electrolytes can be correlated with the extent of surface poisoning by the electrolyte anions or species derived from them. Because from the ATR-FTIR studies, LA was found to adsorb on the Ru surface in the chelating bidentate mode without involving the α-hydroxy groups, it can be concluded that the α-hydroxy group does not facilitate the hydrogenation of LA (and other α-hydroxy acids) by forming a more stable adsorbed intermediate or by influencing the initial adsorption of LA, but it may indirectly increase the hydrogenation rate relative to simple alkanoic acids by facilitating the adsorption of water on the metal surface through the formation of hydrogen bonds. This might be expected from the fact that in the chelating bidentate mode, the LA is adsorbed with the –O–H groups exposed to the solution. It was also determined that chloride does not inhibit the adsorption of LA or hydrogen, and that the enhancement of the ECH rate in HCl may be due to partial desorption of chloride from the electrode surface at longer times and subsequent adsorption of water molecules, which play an important role in ECH. In future work, a more detailed picture of the effect of anion adsorption on LA conversion may be obtainable using in situ Raman spectroscopic studies with Ru single-crystal electrodes to determine the exact mode of adsorption and the nature of surface sites occupied by each type of anion.

Acknowledgments

The authors gratefully acknowledge the Biochemistry Mass Spectrometry Laboratory at Michigan State University for help in the characterization of the products of electrocatalysis by ESI-MS. They are also grateful to Professor Hughes Menard from the University of Sherbrooke, Sherbrooke, QC, who developed the electrocatalytic hydrogenation method using RVC electrodes, for his generous help and advice. Financial support was provided by National Science Foundation grant CTS-0328112.

Supporting information

The online vision on this article contains additional supplementary material.

Please visit doi: 10.1016/j.jcat.2006.11.009.

References

[1] (a) Z. Zhang, J.E. Jackson, D.J. Miller, Appl. Catal. A 219 (2001) 89;
(b) Z. Zhang, J.E. Jackson, D.J. Miller, Ind. Eng. Chem. Res. 41 (2002) 691.
[2] (a) F.T. Jere, D.J. Miller, J.E. Jackson, Org. Lett. 5 (2003) 527;
(b) F.T. Jere, J.E. Jackson, D.J. Miller, Ind. Eng. Chem. Res. 43 (2004) 3297.
[3] F. Laplante, L. Brossard, H. Menard, Can. J. Chem. 81 (3) (2003) 258.
[4] (a) H. Ilikti, N. Rekik, M.J. Thomalla, J. Appl. Electrochem. 32 (2002) 603;
(b) H. Ilikti, N. Rekik, M.J. Thomalla, J. Appl. Electrochem. 34 (2004) 127.
[5] A.K. Cheong, Y. Bolduc, J. Lessard, Can. J. Chem. 71 (1993) 1850.
[6] B. Mahdavi, P. Chambrion, J. Binette, E. Martel, J. Lessard, Can. J. Chem. 73 (1995) 846.
[7] A.M. Polcaro, S. Palmas, S. Dermini, Ind. Eng. Chem. Res. 32 (1993) 1315.
[8] J. Farrugia, unpublished work.
[9] A. Cyr, F. Chiltz, P. Jeanson, A. Martel, L. Brossard, J. Lessard, H. Menard, Can. J. Chem. 78 (2000) 307.
[10] P. Dabo, A. Cyr, J. Lessard, L. Brossard, H. Menard, Can. J. Chem. 77 (1999) 1225.
[11] L. Ruest, H. Menard, V. Moreau, F. Laplante, Can. J. Chem. 80 (2002) 1662.
[12] P. Dube, F. Kerdouss, P. Proulx, L. Brossard, H. Menard, J. Appl. Electrochem. 33 (2003) 541.
[13] H. Miyake, S. Ye, M. Osawa, Electrochem. Commun. 4 (2002) 973.
[14] L.A. Curtiss, K. Raghavachari, P.C. Redfern, V. Rassolov, J.A. Pople, J. Chem. Phys. 109 (1998) 7764.
[15] M.J. Frisch, G.W. Trucks, H.B. Schlegel, G.E. Scuseria, M.A. Robb, J.R. Cheeseman, V.G. Zakrzewski, J.A. Montgomery Jr., R.E. Stratmann, J.C. Burant, S. Dapprich, J.M. Millam, A.D. Daniels, K.N. Kudin, M.C. Strain, O. Farkas, J. Tomasi, V. Barone, M. Cossi, R. Cammi, B. Mennucci, C. Pomelli, C. Adamo, S. Clifford, J. Ochterski, G.A. Petersson, P.Y. Ayala, Q. Cui, K. Morokuma, D.K. Malick, A.D. Rabuck, K. Raghavachari, J.B. Foresman, J. Cioslowski, J.V. Ortiz, A.G. Baboul, B.B. Stefanov, G. Liu, A. Liashenko, P. Piskorz, I. Komaromi, R. Gomperts, R.L. Martin, D.J. Fox, T. Keith, M.A. Al-Laham, C.Y. Peng, A. Nanayakkara, C. Gonzalez, M. Challacombe, P.M.W. Gill, B.G. Johnson, W. Chen, M.W. Wong, J.L. Andres, M. Head-Gordon, E.S. Replogle, J.A. Pople, Gaussian 98 (Revision A.7), Gaussian, Inc., Pittsburgh, PA, 1998.
[16] (a) S. Miertus, E. Scrocco, J. Tomasi, J. Chem. Phys. 55 (1981) 117;
S. Miertus, J. Tomasi, Chem. Phys. 65 (1982) 239;
(b) M. Cossi, V. Barone, R. Cammi, J. Tomasi, Chem. Phys. Lett. 255 (1996) 327;
(c) V. Barone, M. Cossi, J. Tomasi, J. Comput. Chem. 19 (1998) 404.
[17] K.P. Nambiar, D.M. Stauffer, P.A. Kolodziej, S.A. Benner, J. Am. Chem. Soc. 105 (1983) 5886.
[18] X.E. Hu, H.W. Yang, X.J. Wang, R.S. Bai, J. Appl. Electrochem. 32 (2002) 321.
[19] K. Amouzegar, O. Savadogo, Electrochim. Acta 39 (4) (1994) 557.
[20] A. Roessler, O. Dossenbach, P. Rys, J. Electrochem. Soc. 150 (1) (2003) D1.
[21] A. Bryan, J. Grimshaw, Electrochim. Acta 42 (13–14) (1997) 2101.
[22] Y. Senda, M. Tateoka, H. Itoh, J. Ishiyama, Bull. Chem. Soc. Jpn. 64 (1991) 3302.
[23] H. Nielsen, P.E. Sorensen, Acta Chem. Scand. A 31 (1977) 739.
[24] E. Lamy-Pitara, S. El Mouahid, J. Barbier, Electrochim. Acta 43 (2000) 4299.
[25] G. Horanyi, Electrochim. Acta 36 (1991) 1453.
[26] S. Hadzi-Jordanov, H. Angerstein-Koziowska, M. Yukovic, B.E. Conway, J. Phys. Chem. 81 (24) (1977) 2271.
[27] Y. Sawatari, J. Inukai, M. Ito, J. Electron Spectrosc. Relat. Phenom. 64/65 (1993) 515.
[28] N. Hoshi, M. Kuroda, T. Ogawa, O. Koga, Y. Hori, Langmuir 20 (2004) 5066.
[29] Y. Shingaya, M. Ito, Electrochim. Acta 37 (1992) 365.
[30] F. Colom, M.J. Gonzalez-Tejera, J. Electroanal. Chem. 190 (1985) 243.
[31] N.S. Marinkovic, J.X. Wang, H. Zajonz, R.R. Adzic, J. Electroanal. Chem. 500 (1–2) (2001) 388.
[32] Y. Shingaya, M. Ito, J. Electroanal. Chem. 467 (1999) 299.
[33] A. Ahmadi, R.W. Evans, G. Attard, J. Electroanal. Chem. 350 (1993) 279.
[34] G. Horanyi, E.M. Rizmayer, J. Electroanal. Chem. 181 (1984) 199.
[35] M. Osawa, M. Ikeda, J. Phys. Chem. 95 (1991) 9914.
[36] K. Ataka, T. Yotsuyanigi, M. Osawa, J. Phys. Chem. 100 (1996) 10664.
[37] K. Ataka, M. Osawa, Langmuir 14 (1998) 951.
[38] E. Pretsch, J. Seibl, D. Clerc, W. Simon, Tables of Spectral Data for Structure Determination of Organic Compounds, second ed., Springer-Verlag, 1985, p. I85.
[39] (a) P.A. Thiel, E.M. Hoffman, W.H. Weinberg, J. Chem. Phys. 75 (1981) 5556;

(b) P.A. Thiel, R.A. DePaola, W.H. Weinberg, J. Chem. Phys. 80 (1984) 5326.
[40] G. Brink, M. Falk, Can. J. Chem. 48 (1970) 2096.
[41] (a) G.E. Walrafen, J. Chem. Phys. 36 (1962) 1035;
(b) G.E. Walrafen, J. Chem. Phys. 55 (1971) 768.
[42] F. Kitamura, N. Nanbu, T. Ohsaka, K. Tokuda, J. Electroanal. Chem. 452 (1998) 241.
[43] P. Vassilev, R.A. Van Santen, M.T.M. Koper, J. Chem. Phys. 122 (2005) 054701.
[44] K. Kunimatsu, H. Uchida, M. Osawa, M. Watanabe, J. Electroanal. Chem. 587 (2006) 299.
[45] K. Kunimatsu, T. Senzaki, M. Tsushima, M. Osawa, Chem. Phys. Lett. 401 (2005) 451.
[46] T. Yokoyama, N. Yamagata, Appl. Catal. A Gen. 221 (2001) 227.
[47] L. Peereboom, unpublished results.
[48] R.D. Cortright, M. Sanchez-Castillo, J.A. Dumesic, Appl. Catal. B 39 (2002) 353.
[49] R.D. Cortright, J.A. Dumesic, Adv. Catal. 46 (2001) 161.
[50] M. Falorni, G. Giacomelli, A. Porcheddu, M. Taddei, J. Org. Chem. 64 (1999) 8962.
[51] D.G. Kovacs, in preparation.